

Discovery of Superior Cu-GaO_x-HoO_y Catalysts for the Reduction of Carbon Dioxide to Methanol at Atmospheric Pressure

Bahman Zohour,^[a] Iskender Yilgor,^[b] Mehmet A. Gulgun,^[c] Ozgur Birer,^[b] Ugur Unal,^[b] Craig Leidholm,^[d] and Selim Senkan^{*[a]}

Catalytic conversion of carbon dioxide to liquid fuels and basic chemicals by using solar-derived hydrogen at, or near, ambient pressure is a highly desirable goal in heterogeneous catalysis. If realized, this technology could lead to a more sustainable society together with decentralized power generation. A novel class of holmium-containing multi-metal oxide Cu catalysts, discovered through the application of high-throughput methods, is reported. In particular, ternary systems of Cu-GaO_x-HoO_y > Cu-CeO_x-HoO_y ~ Cu-LaO_x-HoO_y, supported on γ-Al₂O₃ exhibited superior methanol production (10×) with less CO formation than previously reported catalysts at 1 atm pressure. Holmium was shown to be highly dispersed as few-atom clusters, suggesting that the formation of trimetallic sites could be the key for the promotion of methanol synthesis by Ho.

Efficient catalytic reduction of carbon dioxide, the primary product of the combustion of fossil fuels and an increasing atmospheric greenhouse gas, to methanol represents an important step towards the creation of a sustainable society. Methanol has been proposed both as a chemical feedstock as well as a convenient liquid medium of energy storage.^[1–4] Although the CO₂ reduction process requires molecular hydrogen, it can easily be obtained by the electrolysis of water by using electricity obtained from photovoltaic cells or wind turbines.^[5–8]

Once produced, methanol can be transformed into a wide range of useful chemicals, such as dimethyl ether (DME), ethylene, gasoline, diesel, and others by using established technologies.^[1–3] In addition, methanol can also be used directly in

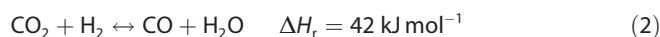
combustion engines and fuel cells, thereby allowing the continuous generation of electricity and enabling energy sustainability.

Currently, methanol is produced exclusively from syngas (CO/CO₂/H₂) obtained from the reforming of fossil fuels in centralized facilities, over Cu-ZnO catalysts promoted by Al₂O₃ at 50–100 bar (1 bar = 0.1 MPa) and 200–300 °C.^[9–15] This catalyst is also active for the water-gas-shift reaction.^[16–19] Owing to the practical importance of this technology, catalysts for methanol synthesis have been studied extensively and optimized for use with syngas at high pressures. Most catalysts investigated to date for the title reaction are based on the Cu-ZnO-Al₂O₃ system modified by metals such as Zr, Ga, Si, Al, B, Cr, V, Ti, and others.^[20] Although high methanol yields have been reported at a pressure of 360 bar,^[21] Cu-ZnO-Al₂O₃ system could not be used efficiently for neat CO₂ reduction at low pressures.^[22] This finding demonstrated the need for the discovery and optimization of new and more active catalysts for methanol synthesis. Recently, a Ni-Ga/SiO₂ system prepared by the standard impregnation technique was reported to give methanol yields that were comparable to the traditional Cu-ZnO-Al₂O₃ catalysts prepared by co-precipitation at atmospheric pressure.^[22] In another recent report, also at 1 atm, CeO_x deposited on Cu(111) and Cu-CeO_x co-deposited on TiO₂(110) surfaces (by chemical vapor deposition) produced significantly more CH₃OH than the Cu-ZnO(0001) surfaces.^[23] A hybrid oxide catalyst comprising MnO_x nanoparticles supported on mesoporous Co₃O₄ was also recently reported to exhibit significant CH₃OH production at a higher pressure of 4 bar, together with CO and hydrocarbon products.^[24]

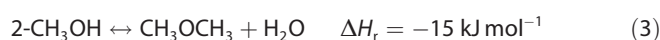
Methanol formation from carbon dioxide and hydrogen proceeds via the following reaction:



This reaction is often accompanied by the reverse water-gas-shift reaction (RWGS):



In the presence of acidic surfaces, for example, H-ZSM5 or γ-Al₂O₃, the CH₃OH produced is readily converted to DME, which is also a desirable product, by dehydration:^[9,10,25]



Herein, we report the discovery of a series of superior and novel holmium-containing catalytic materials for the low-pressure reduction of CO₂ to CH₃OH and DME. By using impregna-

[a] B. Zohour, Prof. Dr. S. Senkan
Department of Chemical Engineering
University of California
Los Angeles, CA (USA)
E-mail: ssenkan@gmail.com

[b] Prof. Dr. I. Yilgor, Prof. Dr. O. Birer, Prof. Dr. U. Unal
Department of Chemistry, KUYTAM
Koc University
Sariyer, Istanbul (Turkey)

[c] Prof. Dr. M. A. Gulgun
Department of Material Science and Engineering
Sabanci University
Tuzla, Istanbul (Turkey)

[d] C. Leidholm
Laboratory Catalyst Systems, LLC
Los Angeles, CA (USA)

Supporting Information for this article can be found under <http://dx.doi.org/10.1002/cctc.201600020>.

tion and high-throughput (HT) catalyst-screening technologies developed in our laboratories,^[26,27] we systematically investigated the oxides of single, binary, and ternary combinations of 27 metals (total metal atom loading of 20 wt %) with several support materials in over 3000 experiments. Our studies led to the discovery of γ -Al₂O₃-supported Cu-GaO_x-HoO_y as well as Cu-CeO_x-HoO_y and Cu-LaO_x-HoO_y systems, which exhibit superior methanol production and less CO formation than other materials reported in the literature. The observed higher activity and selectivity of the Cu-Ga-Ho system could be related to the formation of trimetallic active sites.

Initial screening experiments led to the determination of a number of binary systems that exhibited catalytic activity for CH₃OH synthesis mostly over the γ -Al₂O₃ support. These binary systems, in decreasing order of CH₃OH production at 260 °C were: Cu-Ga^[14,28] > Cu-La^[29] ~ Cu-Ce^[23] > Cu-Ho ~ Cu-Zr^[15] > Ga-Ni/SiO₂^[22] ~ Cu-Zn^[10,12,13] ~ Ga-Ho ~ Cu-Mg > Zn-Ir, which are consistent with the literature. The validity of our experimental approach is supported by the observation that the relative performances of our as-prepared Cu-Zn/Al₂O₃ and Ga-Ni/SiO₂ catalysts are similar to one another, a finding that is identical to results reported by Studt et al. who used co-precipitation to synthesize the traditional Cu-Zn-Al₂O₃ catalysts.^[22] The higher-performing binary systems were then used as the basis to explore the ternary systems at different loadings and temperatures. In Figure 1, the reactor exit mole percentages for CH₃OH ($\times 10^4$), DME ($\times 10^4$), and CO ($\times 0.5 \times 10^3$) are presented for the Ho-containing ternary catalysts with the best performance together with selected binary systems for comparison. The values presented in Figure 1 correspond to the average of three different sets of experiments that were within 10% of each other. It should be noted that CO₂ conversions, thus product mole fractions, were small because of the high gas velocities used (GHSV $\approx 200\,000$ h⁻¹). The high gas velocities allowed the catalysts to remain isothermal, which enabled the undertaking of rigorous comparisons of their intrinsic activities. The results reported herein must be studied in greater detail to better understand the catalyst structures, activities, selectivities, reaction mechanisms, and optimization of their performances.

From Figure 1a it can be seen that our HT experiments produced the following order for CH₃OH production for some of the previously reported catalysts at 260 °C: Cu-Ga₂O₃ (3)^[14,28] > Cu-La₂O₃ (9)^[29] > Cu-CeO₂ (11)^[23] > Cu-Zn-(Zr-Al₂O₃) (7)^[15,30] > Cu-ZrO₂ (6)^[15] > Ga-Ni/SiO₂ (13)^[22] ~ MnO_x/m-Co₃O₄ hybrid (16)^[24] ~ Cu-ZnO₂/Al₂O₃ (1)^[10,12,13] Unlike the reported high performance at 4 bar, the methanol production of the hybrid MnO_x/m-Co₃O₄ catalyst (16)^[24] was surprisingly poor at 1 atm, only on par with the as-prepared Cu-Zn/Al₂O₃ (1) ~ Ga-Ni/SiO₂ (13) systems (see Figure 1a); nevertheless, 16 was a very active catalyst producing very high levels of CO and CH₄ along with some C₂H₄ and higher hydrocarbons (C₃₊).

As evident from Figure 1, our γ -Al₂O₃-supported ternary Cu-GaO_x-HoO_y catalyst (4, Cu-Ga-Ho at 8-8-4 metal wt %) together with the Cu-LaO_x-HoO_y (10, Cu-La-Ho at 10-5-5 metal wt %) and Cu-CeO_x-HoO_y (12, Cu-Ce-Ho at 10-5-5 metal wt %) systems significantly outperform the previously reported systems.

For example, at 260 °C (Figure 1a), the Cu-GaO_x-HoO_y catalyst (4) produced CH₃OH at 1.14×10^{-4} %, which is about a factor of 10 higher than the Cu-Zn/Al₂O₃ system (1) of 0.112×10^{-4} %, while producing similar levels of CO. It is also important to note that catalyst 4 also produced significant levels of DME. In fact, if we were to combine the yields for DME ($2 \times 0.42 \times 10^{-4} = 0.84 \times 10^{-4}$) and CH₃OH (1.14×10^{-4}) (4), at 260 °C, the performance of catalyst 4 would be a factor of 17 higher than that of catalyst 1 and 13. These results correspond to a CH₃OH + DME selectivity of 48% for the Cu-GaO_x-HoO_y (4) catalyst at 260 °C. The turnover frequency (TOF) of catalyst 4 was estimated to be approximately 1.6×10^{-4} s⁻¹ at 260 °C (Figure 1a) for the combined production of CH₃OH and DME; this was calculated by assuming ≈ 7 nm diameter spherical Cu metal clusters ($\approx 20\,000$ Cu atoms) and ≈ 3000 surface atoms exposed for reaction and 10% reactant gas utilization.^[27] Similar considerations for the Cu-Zn/Al₂O₃ catalyst (1) result in a TOF value of 0.45×10^{-5} s⁻¹, which is in agreement with the values reported in literature.^[22,24]

Holmium also had a dramatic promotional effect on some of the reported binary CH₃OH catalyst systems. For example, both CH₃OH and DME production increased significantly by the Ho doping of catalyst 1 by more than a factor of two (2) at 300 °C. For the case of the Cu-CeO₂ (11), Ho doping was also influential, increasing CH₃OH levels by approximately a factor of two (12) at 260 °C. However, Ho did not promote CH₃OH formation in the Ga-Ni/Al₂O₃ system (15), although it significantly increased CO and CH₄ (not included in Figure 1) production.

Increasing the temperature from 260 to 280 °C significantly increased CH₃OH production for the Cu-GaO_x-HoO_y (4) catalyst. However, increasing the temperature further from 280 to 300 °C resulted in a smaller increase in CH₃OH formation. This result is not surprising in view of the equilibrium considerations of this exothermic reaction [Eq (1)].^[31] On the other hand, increasing the temperature increased the CO production substantially, clearly demonstrating the need to develop low-temperature catalysts for the synthesis of CH₃OH from CO₂.

Rapid decreases in CH₃OH production were observed within few hours with the Cu-Zn/Al₂O₃ (1) catalyst. None of the γ -Al₂O₃-supported Cu-GaO_x-HoO_y (4), Cu-LaO_x-HoO_y (10), or Cu-CeO_x-HoO_y (12) exhibited any significant deactivation or change in methanol selectivity during ≈ 10 h of continuous runs or after repeated reduction–reaction cycles. The time-on-stream performance of the Cu-GaO_x-HoO_y (4) catalyst presented in Figure 2 at 260 °C shows that the combined selectivities for CH₃OH and DME remained at approximately 48% for the entire 10 h testing period.

In the Cu-Zn/Al₂O₃ system (1), the metallic copper clusters are accepted to be the sites for methanol synthesis, whereas ZnO has been proposed to act both as a physical promoter (i.e., to assist in the formation of a larger number of surface Cu sites) and as a promoter for the Cu-ZnO synergy.^[11] The same Cu-ZnO sites are also believed to be catalysts for the RWGS reaction. It is also widely accepted that CH₃OH production from CO₂ over Cu-ZnO catalysts occurs via the formation of surface formates $\text{HCOO-M} \rightarrow \text{HCOOH-M} \rightarrow \text{CH}_3\text{O}_2\text{-M} \rightarrow \text{CH}_2\text{O-M} \rightarrow \text{CH}_3\text{O-M} \rightarrow \text{CH}_3\text{OH-M}$.^[31]

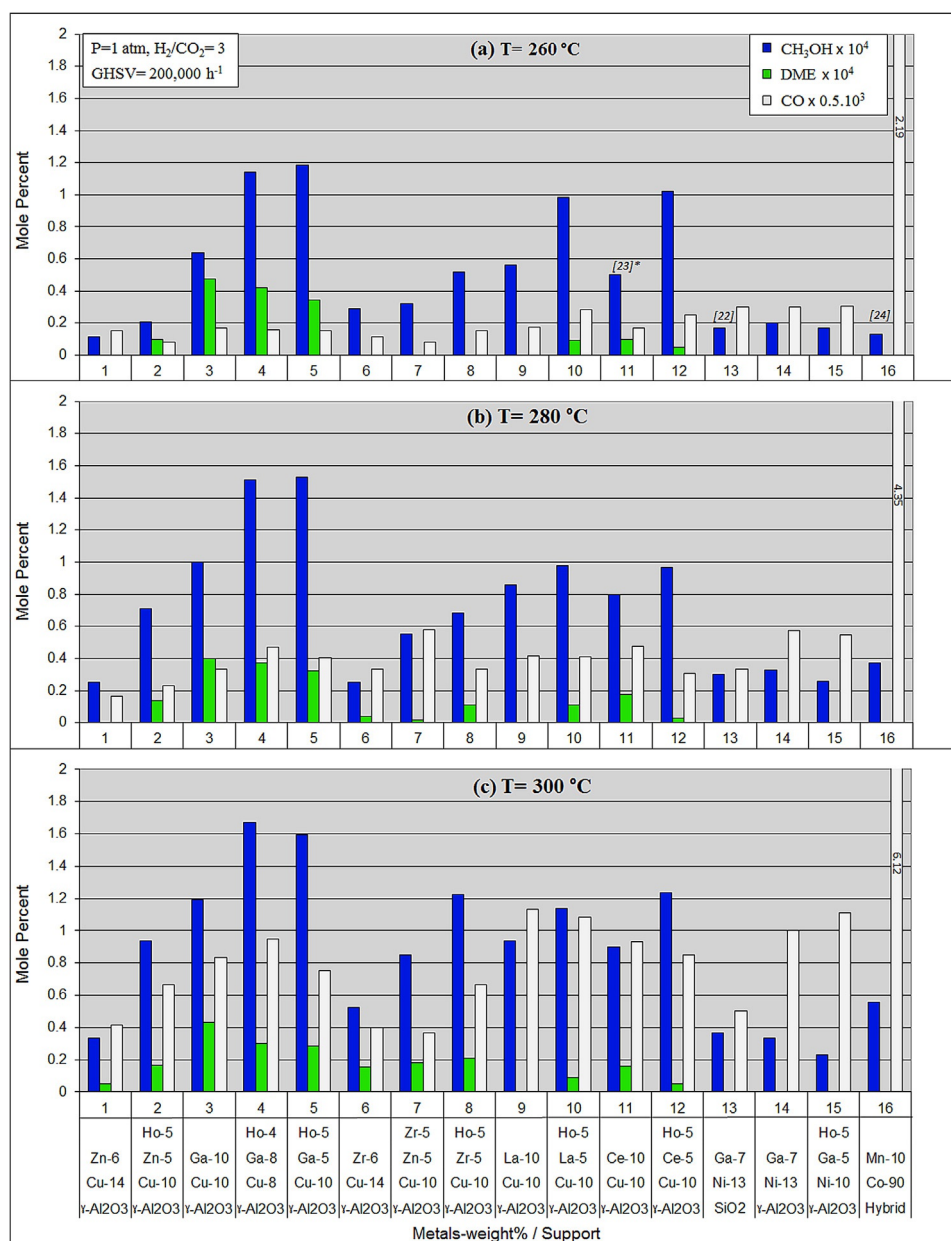


Figure 1. Reactor exit CH₃OH, DME, and CO mol% levels for the high-performing Ho-containing catalysts together with some previously reported catalytic systems at a) 260 °C, b) 280 °C, and c) 300 °C. Significant amounts of CH₄ were also produced with the Ni-containing catalysts (13, 14, 15) and for 16, but are not presented for clarity. [n]* refers to catalytic materials reported recently in the literature at low pressures.

For the Ni-Ga/SiO₂ system (13), the Ga-rich sites have been reported to facilitate methanol synthesis, whereas the Ni-rich sites have been suggested to be responsible for the RWGS and methanation reactions.^[22] Consequently, the superior performance of the Cu-GaO_x-HoO_y system (4), which contains both Cu and Ga sites, can be due, in part, to their mutual physical and chemical promotion (3). The remarkable effect of Ho in the promotion of methanol synthesis could be attributed to the formation of very small clusters that are highly dispersed. As discussed in the characterization section below, STEM images of catalyst 4 showed the presence of few-atom (1–3 atom) Ho clusters. Some of these clusters also appear to be

positioned along the Cu and Ga cluster interfaces or on the surfaces of their alloys, creating trimetallic sites that could be the key for the promotion of methanol synthesis by Ho. This representation is also supported by the experimentally observed order of activity of the CH₃OH catalysts, that is, Cu-Ga-Ho (4) > Cu-Ga (3) > Cu-Ho > Ga-Ho.

The reduced Cu-GaO_x-HoO_y system was characterized (4, Cu-Ga-Ho at 8-8-4 metal wt% loading and 5.3/4.8/1 atom ratio) by using BET analysis (Micromeritics ASAP 2020 using N₂), scanning transmission electron microscopy (STEM, JEOL, JEM-ARM200CFEG UHR, with EDS), X-ray diffraction (XRD) (Bruker Xflash 5010), and X-ray photoelectron (XPS) (ThermoScientific

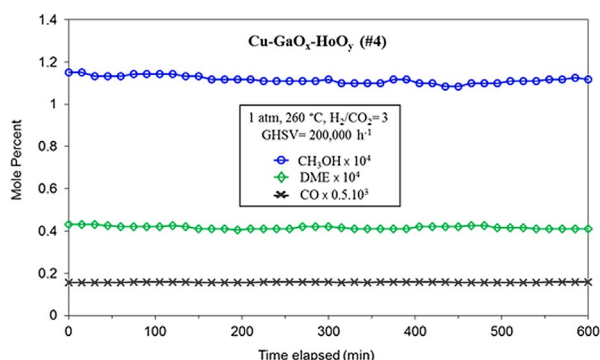


Figure 2. Time-on-stream behavior of the Cu-Ga₂O₃-Ho₂O₃ (4) catalyst shows no significant performance change over a 10 h testing period.

K-Alpha) spectroscopy to develop insights on its structure and surface chemistry. BET analysis indicated a surface area of 142 m² g⁻¹ for the catalyst, consistent with the alumina support. The XRD spectra (see the Supporting Information) only showed the features of the Al₂O₃ support, suggesting the presence of amorphous Cu, Ga, and Ho moieties or their nanosize crystallites. This finding was also confirmed by the high-resolution TEM studies (Figure 3); HR-TEM images of the reduced catalyst 4 (Cu-Ga-Ho at 8–8–4 wt% metal loading and atom ratios of 5.2/4.8/1) is provided in Figures 3a and 3b. Element mapping images obtained from STEM/EDS indicate the presence of 5–7 nm Ga (Figure 3e) and Cu (Figure 3f) clusters in close proximity to one another, which also suggests the possibility of some alloy formation. On the other hand the Ho map did not show the presence of larger particles (Figure 3c). The high angular annular dark field (HAADF) Z-contrast ($\sim z^2$) image indicated that the heavy Ho ($z=165$) is highly dispersed and exists only as few-atom (1–3 atom) clusters (Figure 3d).

Ex situ XPS studies of the reduced catalyst 4 indicated the presence of both Cu⁰ and CuO, whereas only Ga₂O₃ and Ho₂O₃ were observed at the surface (see the Supporting Information). Some oxidation of Cu was observed because of exposure to the atmosphere during sample transfer to the XPS system. Consequently, Cu-Ga₂O₃-Ho₂O₃ could be the correct representation of catalyst 4. It is interesting to note that the surface concentration of Ga was higher, whereas those for Cu and Ho were lower, than their nominal/bulk values for the Cu-Ga₂O₃-Ho₂O₃ (4) catalyst. Further characterizations, as well as detailed kinetic and quantum modeling studies, are underway to better understand the nature of the active site(s) and to explain the mechanism of action of the novel Cu-Ga₂O₃-Ho₂O₃ system in the promotion of CH₃OH synthesis from CO₂ and H₂.

In summary, high-throughput impregnation synthesis and reaction screening of the binary and ternary combinations of 27 metals and 5 supports for the hydrogenation of CO₂ to CH₃OH under atmospheric pressure led to the discovery of a novel class of superior ternary catalytic materials containing holmium, while reproducing the trends for the relative performances of the already established binary catalytic systems from the literature. The Cu-Ga₂O₃-Ho₂O₃/γ-Al₂O₃ system exhibited the highest CH₃OH production together with significant levels of DME formation, and maintained its activity and selectivity over a long period of time. Considering the significant practical interest of these processes for a sustainable chemical industry and society in general, the newly discovered catalytic materials reported herein require further investigations to better understand the nature of the active sites, optimize their synthesis and operating conditions, including studies at higher pressures, to increase CH₃OH and DME yields.

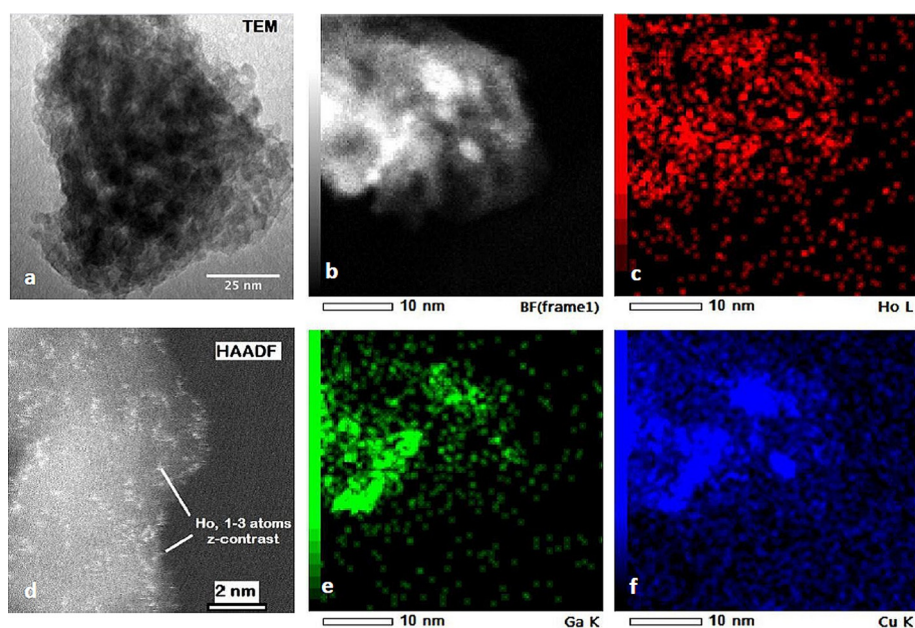


Figure 3. a, b) HR-TEM images of the reduced catalyst 4 (Cu-Ga-Ho at 8–8–4 wt% metal loading and atom ratios of 5.2/4.8/1). c, d) STEM-EDS images of the element maps of Ho, e) Ga, and f) Cu over γ-Al₂O₃.

Experimental Section

The catalysts were prepared by impregnation of powders of γ - Al_2O_3 , CeO_2 , SiO_2 , TiO_2 , and Y-ZrO_2 with single, binary, and ternary mixtures of aqueous (nitrate) salt solutions of 27 metals: Li, Na, Rb, Cs, Mg, Ca and Sr, Ga, V, Cr, Mn, Co, Ni, Cu, Zn, Zr, Ru, Ir, Ag, Au, La, Ce, Pr, Dy, Ho, Er, and Yb. Systematic consideration of different metal ratios and loadings necessitated the preparation of approximately 3000 distinct catalytic materials. For example, the best-performing trimetallic ($\text{Cu-GaO}_x\text{-HoO}_x/\gamma\text{-Al}_2\text{O}_3$, **4**) catalysts were prepared as follows: A predetermined amount of $\gamma\text{-Al}_2\text{O}_3$ support (Alfa Aesar, surface area of $\approx 150\text{ m}^2\text{ g}^{-1}$) was soaked in an aqueous solution of $\text{Cu}(\text{NO}_3)_2 \cdot 2.5\text{ H}_2\text{O}$, $\text{Ga}(\text{NO}_3)_3 \cdot 6\text{ H}_2\text{O}$, and $\text{Ho}(\text{NO}_3)_3 \cdot 5\text{ H}_2\text{O}$ (Alfa Aesar) at concentrations previously determined to yield the desired metal loadings. The mixture was then dried at 120°C while stirring, followed by calcining in air at 450°C for 6 h. In addition, the recently reported hybrid $\text{MnO}_x/\text{m-Co}_3\text{O}_4$ catalyst (**16**) was acquired and tested.^[24]

Catalyst screenings were performed by using a high-throughput (HT) array channel microreactor system, which is shown in Figure 4, details of which have been described previously.^[26,27] The system allows parallel screening of up to 80 catalytic materials. In array microreactors, reactant gases flow over the flat surfaces of compacted powders (20 mg of $\gamma\text{-Al}_2\text{O}_3$ -based and 6 mg of SiO_2 -based) of catalytic materials that are placed into the wells in each reactor channel (see Figure 4 top right inset). Consequently, the majority of the gases exit the reactor while only a small fraction ($\approx 10\%$) participate in the catalytic reaction process.^[27] This arrangement results in the establishment of identical flow rates or contact times in every channel, which enables the rapid comparison of the catalytic performances of up to 80 catalysts in a single experiment. The experiments were performed in the following manner: Firstly, the catalysts were reduced under H_2/He (50/50) flow at a temperature in the range of $230\text{--}350^\circ\text{C}$ for 2 h. Catalysts were then cooled to the desired reaction temperature while still under H_2/He flow, and the gas flow was switched to the reactants. The experiments were performed at 260, 280, and 300°C , at 1 atm pressure and at gas hourly space velocity (GHSV) of approximately $200\,000\text{ h}^{-1}$. The feed gas consisted of 25 vol% CO_2 (Matheson,

99.9% purity) and 75 vol% H_2 (Matheson, 99.99%). Gas sampling was accomplished by withdrawing reactor exit gases by using a passivated 200 micron ID capillary sampling probe that was sequentially positioned into each reactor channel, followed by on-line gas analysis either by mass spectrometry (MS, Stanford Research Systems, RGA-200) or by gas chromatography (Micro-GC Varian, CP-4900). The GC had dual Porapak U (10 m) and molecular sieve 13X (10 m) modules each equipped with individual thermal conductivity detectors (TCD). Using MS analysis the screening of the entire 80-catalyst library typically took 30 min or less depending on the sampling capillary dwell time inside and outside the reactor channels and the mass range and scan rate of the MS.^[26,27] Consequently, MS analysis was used for initial screening to rapidly identify promising leads. The leads were then studied in greater detail by gas chromatography in smaller sets of 10 to 20 catalysts to better compare them under similar time-on-stream conditions. In the present work, each GC analysis took approximately 2.5 min for completion including a 30 s sampling time. The following products were detected and quantified: CH_3OH , CH_3OCH_3 (DME), CO , CH_4 , C_2S , and C_3S . However, only CH_3OH , CH_3OCH_3 (DME), and CO were reported in Figure 1 for clarity.

Acknowledgements

We thank Laboratory Catalyst Systems (LCS), LLC for funding and access to their high-throughput equipment and catalyst data base. We also thank Dr. Selim Alayoglu and Dr. Kwangjin An of the Lawrence Berkeley National Laboratory for providing the hybrid $\text{MgO}_x/\text{CoO}_x$ catalyst. Author contributions: BZ, CL, and SS initiated and performed the original catalyst discovery work at LCS. IY, OB, and UU performed and interpreted the XRD and XPS analysis. MAG performed and interpreted the HRTEM analysis.

Keywords: carbon dioxide • dimethyl ether • heterogeneous catalysis • high-throughput testing • methanol synthesis

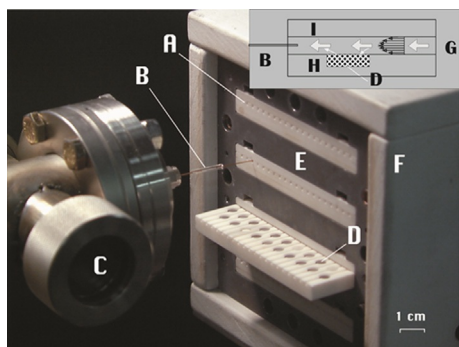


Figure 4. High-throughput microreactor catalyst screening system. A) Reactor bank with 20 parallel channels (4 banks, total 80 channels) micro-machined over a ceramic plate; B) Capillary gas-sampling probe; C) Gas analysis performed by mass spectrometer (MS) or gas chromatograph (GC); D) Wells for the placement of catalyst pellets or powders; E) Temperature-controlled heating block with a preheat zone (not shown); F) Insulation. The top right insert shows the schematic of the side view of a channel reactor: G) Reactant and product gases flow through the channel, which is embedded into the lower ceramic plate (H) and isolated by the cover plate (I). Gases flow over the catalyst bed (D) resulting in minimal pressure drop. The capillary probe (B) is also shown inserted into the channel for sampling.

- [1] G. A. Olah, *Angew. Chem. Int. Ed.* **2005**, *44*, 2636–2639; *Angew. Chem.* **2005**, *117*, 2692–2696.
- [2] G. A. Olah, A. Goepfert, G. S. Prakash, *J. Org. Chem.* **2009**, *74*, 487–498.
- [3] G. A. Olah, A. Goepfert, G. S. Prakash, *Beyond Oil and Gas: The Methanol Economy*, Wiley, Weinheim, **2009**.
- [4] G. A. Olah, *Angew. Chem. Int. Ed.* **2013**, *52*, 104–107; *Angew. Chem.* **2013**, *125*, 112–116.
- [5] N. S. Lewis, D. G. Nocera, *Proc. Natl. Acad. Sci. USA* **2006**, *103*, 15729–15735.
- [6] W. El-Khattam, M. M. A. Salama, *Electr. Power Syst. Res.* **2004**, *71*, 119–128.
- [7] G. Crabtree, J. Sarrao, *Phys. World* **2009**, *22*, 24–30.
- [8] M. Z. Jacobson, M. A. Delucchi, *Energy Policy* **2011**, *39*, 1154–1169.
- [9] G. Bozga, I. T. Apan, R. E. Bozga, *Recent Pat. Catal.* **2013**, *2*, 68–81.
- [10] F. Pontzena, W. Liebner, V. Gronemann, M. Rothaemel, B. Ahlers, *Catal. Today* **2011**, *171*, 242–250.
- [11] M. Behrens, F. Studt, I. Kasatkin, S. Kühl, M. Hävecker, F. Abild-Pedersen, S. Zander, F. Girgsdies, P. Kurr, B. L. Kniep, M. Tovar, R. W. Fischer, J. K. Nørskov, R. Schlögl, *Science* **2012**, *336*, 893–897.
- [12] M. M. Günter, T. Ressler, B. Bems, C. Büscher, T. Genger, O. Hinrichsen, M. Muhler, R. Schlögl, *Catal. Lett.* **2001**, *71*, 37–44.
- [13] M. Behrens, S. Zander, P. Kurr, N. Jacobsen, J. Senker, G. Koch, T. Ressler, R. W. Fischer, R. Schlögl, *J. Am. Chem. Soc.* **2013**, *135*, 6061–6068.
- [14] R. Ladera, F. J. Pérez-Alonso, J. M. González-Carballo, M. Ojeda, S. Rojas, J. L. G. Fierro, *Appl. Catal. B* **2013**, *142*, 241–248.
- [15] S. G. Jadhav, P. D. Vaidya, B. M. Bhanage, J. B. Joshi, *Chem. Eng. Res. Des.* **2014**, *92*, 2557–2567.
- [16] F. S. Stone, D. Waller, *Top. Catal.* **2003**, *22*, 305–318.

- [17] I. Nakamura, T. Fujitani, T. Uchijima, J. Nakamura, *Surf. Sci.* **1998**, *400*, 387–400.
- [18] M. Ginés, N. Amadeo, M. Laborde, C. Apesteguía, *Appl. Catal. A* **1995**, *131*, 283–296.
- [19] M. Spencer, *Top. Catal.* **1999**, *8*, 259–266.
- [20] Y. Hartadi, D. Widmann, R. J. Behm, *ChemSusChem* **2015**, *8*, 456–465.
- [21] A. Bansode, A. Urakawa, *J. Catal.* **2014**, *309*, 66–70.
- [22] F. Studt, I. Sharafutdinov, F. Abild-Pedersen, C. F. Elkjær, J. S. Hummelshøj, S. Dahl, I. Chorkendorff, J. K. Nørskov, *Nat. Chem.* **2014**, *6*, 320–324.
- [23] J. Graciani, K. Mudiyanse, F. Xu, A. E. Baber, J. Evans, S. D. Senanayake, D. J. Stacchiola, P. Liu, J. Hrbek, J. F. Sanz, J. A. Rodriguez, *Science* **2014**, *345*, 546–550.
- [24] C. S. Li, G. Melaet, W. T. Ralston, K. An, C. Brooks, Y. Ye, Y.-S. Liu, J. Zhu, J. Guo, S. Alayoglu, G. A. Somorjai, *Nat. Commun.* **2015**, *6*, 6538.
- [25] W. H. Chen, B. J. Lin, H. M. Lee, M. H. Huang, *Appl. Energy* **2012**, *98*, 92–101.
- [26] S. Senkan, *Angew. Chem. Int. Ed.* **2001**, *40*, 312–329; *Angew. Chem.* **2001**, *113*, 322–341.
- [27] S. Senkan, K. Kevin, O. Sukru, *Angew. Chem. Int. Ed.* **1999**, *38*, 2794–2799; *Angew. Chem.* **1999**, *111*, 2965–2971.
- [28] J. Toyir, P. R. de La Piscina, J. L. G. Fierro, N. Homs, *Appl. Catal. B* **2001**, *34*, 255–266.
- [29] D. Andriamasinoro, R. Kieffer, A. Kiennemann, *Appl. Catal. A* **1993**, *106*, 201–212.
- [30] C. Li, X. Yuan, K. Fujimoto, *Appl. Catal. A* **2014**, *469*, 306–311.
- [31] L. C. Grabow, M. Mavrikakis, *ACS Catal.* **2011**, *1*, 365–384.

Received: January 8, 2016

Revised: February 25, 2016

Published online on March 16, 2016
